optica

Erbium dopants in nanophotonic silicon waveguides

Lorenz Weiss,† Andreas Gritsch,† Benjamin Merkel, and Andreas Reiserer*

Quantum Networks Group, Max-Planck-Institut für Quantenoptik, Hans-Kopfermann-Straße 1, D-85748 Garching, Germany and Munich Center for Quantum Science and Technology (MCQST), Ludwig-Maximilians-Universität München, Fakultät für Physik, Schellingstraße 4, D-80799 München, Germany

**Corresponding author: andreas.reiserer@mpq.mpg.de*

Received 26 October 2020; accepted 30 November 2020 (Doc. ID 413330); published 6 January 2021

We perform resonant spectroscopy of erbium implanted into nanophotonic silicon waveguides, finding 1 GHz inhomogeneous broadening and homogeneous linewidths below 0.1 GHz. Our study thus introduces a promising materials platform for on-chip quantum information processing.

https://doi.org/10.1364/OPTICA.413330

Individual dopants and atom-like defects in solids are promising platforms for quantum technology. Among all optically active dopants studied to date, either in silicon [1,2] or in other crystals [3], erbium stands out because it exhibits a coherent transition within the main wavelength band of optical telecommunication. Here, high material transparency ensures compatibility with the mature platform of silicon nanophotonics, and the minimal loss of optical fibers might enable quantum networks that span global distances if sufficient coherence is achieved. In silicate crystals, the ground state coherence of erbium can exceed 1 s [4], and that of the optical transition is among the best in any solid. While this has enabled first quantum information experiments with bulk crystals, the integration into nanophotonic structures is highly desirable. This would not only allow for robust and cost-effective fabrication of devices, but can also enhance the interaction strength between the dopants and single photons, thus overcoming the notoriously small dipolar transition strength of erbium.

Recently, silicon nanostructures on top of yttrium orthosilicate (YSO) [5] have enabled the control of single dopants [6]. However, this and related materials are incompatible with standard complementary metal oxide semiconductor (CMOS) processing and have abundant isotopes with nuclear spins that deteriorate the coherence. In contrast, silicon is an almost spin-free material, and isotopic purification largely eliminates the nuclear spin bath and facilitates ultra-narrow optical linewidths [2]. This makes the direct integration of erbium into silicon nanophotonic structures, as studied in this work, highly promising.

Its low solubility prevents sufficient erbium doping during growth from the melt [7]. Therefore, optical characterization requires epitaxial growth or ion implantation. So far, the resulting two-dimensional samples have precluded resonant spectroscopy. We overcome this limitation by integrating erbium dopants into 0.4 mm long nanophotonic wire waveguides [Fig. 1(a)]. With broadband edge coupling, we detect around 2% of the emitted fluorescence. Even in our weakly doped ($\sim 10^{17}$ cm^{-3}) samples, annealed for 10 min at 10^3 K, this enables resonant fluorescence spectroscopy using 1 ms long excitation pulses. During each pulse, a ∼100 MHz frequency sweep avoids bleaching by persistent spectral hole burning to long-lived spin states. In contrast to previous measurements in silicon [1,7,8], resonant fluorescence spectroscopy is sensitive to all dopants that decay radiatively. We thus observe a completely different spectrum [Fig. 1(b)]. Instead of a terahertz-wide distribution, we find only a few sharp Lorentzian peaks, as expected for crystals with low defect concentration. Their inhomogeneous linewidth ranges from 1 to 4 GHz FWHM [Fig. 1(c), blue], and is further reduced in a magnetic field of 0.2 T, in which the peaks split into up to 12 lines depending on the site. The observed width is similar to that in YSO when coupled to nanostructures [6], and its narrowness indicates dopant integration at well-defined lattice sites while preserving the crystalline structure. This is a key step towards quantum controlled applications of erbium-doped silicon.

The presence of several distinct sites might be caused by erbium forming complexes with other impurities, such as oxygen [7]. By changing the annealing procedure, using purer starting material, or co-implanting other dopants, we expect that the number, position, and relative height of the resonances can be engineered. As in other host crystals, the remaining inhomogeneous broadening of the lines is attributed to random strain fields in the waveguide. We expect that—similar to other emitters in silicon [2]—the broadening can be further reduced in isotopically purified samples, opening exciting prospects for ultra-narrow optical lines in nanophotonic structures.

After characterizing the linewidth, we measure the fluorescence lifetime after the excitation laser is switched off. We observe an exponential decay of ∼1 ms on every peak [Fig. 1(c), red]. Compared to other erbium host materials [4–6], this constitutes a reduction by an order of magnitude that holds promise for an enhanced light–matter interaction strength. Remarkably, magnetic dipole transitions can be held responsible for the major part of this decay, as their expected lifetime in silicon is around 1.5 ms [9] and thus close to the measured value. While photonic crystal waveguides and cavities may further shorten the lifetime, using erbium-doped silicon in advanced quantum networking protocols will still require small homogeneous and spectral diffusion linewidths, which we investigate next.

Our measurement technique is based on transient spectral hole burning. Because of saturation, the fluorescence signal S

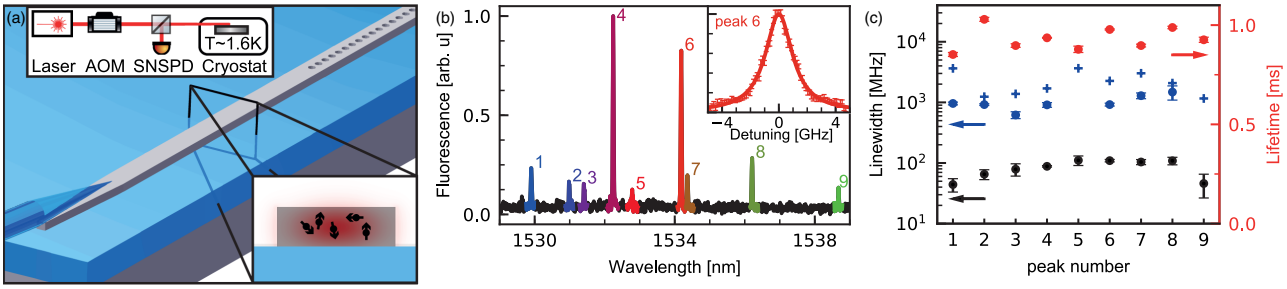

Fig. 1. (a) Experimental setup. A 220 × 700 nm small silicon waveguide (gray) is terminated by a broadband photonic crystal mirror, fabricated on a commercial silicon-on-insulator chip (blue). Efficient broadband coupling is achieved with a tapered fiber touching the waveguide (blue). The bottom inset shows a cross section. Erbium (black arrows) has been implanted into the fundamental guided mode (red). The top inset shows a sketch of the setup. A tunable laser is pulsed via two acousto-optical modulators (AOM) before exciting the dopants. The emitted fluorescence is detected using a single-photon detector (SPD). (b) Fluorescence measurement. We observe nine narrow fluorescence peaks in the telecom C-band, all of which are well fit by Lorentzian curves (inset). (c) Optical properties. Using pulsed resonant spectroscopy, we measured the fluorescence lifetime (red), homogeneous linewidth (black), and inhomogeneous broadening (blue) with (dots) and without (crosses) magnetic field for all observed sites.

increases nonlinearly with the laser intensity I at a single frequency, $S \propto \sqrt{I}$. We therefore apply three laser fields of about the same intensity I, generated at equidistant frequency separation within the inhomogeneous linewidth by electro-optical modulation of the excitation laser. If the separation of the three lines is larger than both the homogeneous and the spectral diffusion linewidth, the signal will increase threefold compared to that of a single field. For small detunings, however, the signal will increase by only $\sim\sqrt{3}$. Thus, by scanning the modulation frequency, we can upper-bound the homogeneous and spectral diffusion linewidth on the timescale of the radiative lifetime.

Again, we preclude detrimental effects of persistent spectral hole burning by slightly changing the laser frequency between repetitions of the experiment. Inverted Lorentzian fits to the data give a spectral diffusion linewidth between 45 and 110 MHz for the individual erbium sites [Fig. 1(c), black]. The value observed in nanophotonic silicon is thus about four times larger than in nanocavity-coupled YSO [6]. We can exclude dipolar interactions with other magnetic moments in the crystal as a broadening mechanism, as both our dopant concentration and the interaction with the nuclear spin bath is too small. Thus, we attribute the measured spectral diffusion to the proximity of interfaces, a common issue for all solid-state quantum emitters [3] including erbium in other hosts [5,6]. At the used intensity, two-photon absorption should generate about 10^4 free carriers in the waveguide during each excitation pulse. This can change the state of charge traps caused by crystalline defects and dangling bonds at the surface, leading to fluctuating electric fields at the position of the dopant and thus a broadening of the line via the Stark effect. In our samples, the maximum distance of the dopants to the closest interface is around 100 nm. With typical erbium Stark coefficients of 100 Hz · m/V, the expected frequency shift for a single fluctuating charge trap at this distance is tens of megahertz, matching our observations. In future devices, spectral diffusion may therefore be reduced by using waveguides of larger dimension and surface termination (e.g., by hydrogenation). In addition, stabilizing the state of charge traps by applying strong electric fields seems highly promising.

In summary, we have introduced erbium-doped silicon nanophotonics as a novel materials platform for quantum technology. Well-established fabrication techniques should allow for the realization of robust, low-cost, and multiplexed quantum devices. Applications will profit from an increased optical depth in longer waveguides when using an optimized implantation procedure. Alternatively, the dopant interaction with light can be enhanced with resonators. In ultra-high-Q photonic crystal cavities [10], we expect a Purcell enhancement by six orders of magnitude. This would not only bring the system into the strong-coupling regime of cavity quantum electrodynamics, but also shorten the radiative decay to the nanosecond range, such that the lifetime-limited linewidth is of the same order as the spectral diffusion linewidth we observed. Thus, we expect that erbium-doped silicon can be used as an optical interface of single spin qubits operating in the telecom C-band. This offers unique promise for cavity-based quantum networks and distributed quantum information processors based on a scalable platform.

Funding. European Research Council (757772); Deutsche Forschungsgemeinschaft (EXC-2111-390814868); Daimler und Benz Stiftung.

Disclosures. The authors declare no conflicts of interest.

†These authors contributed equally to this work.

REFERENCES

1. C. Yin, M. Rancic, G. G. de Boo, N. Stavrias, J. C. McCallum, M. J. Sellars, and S. Rogge, Nature **497**, 91 (2013).
2. L. Bergeron, C. Chartrand, A. T. K. Kurkjian, K. J. Morse, H. Riemann, N. V. Abrosimov, P. Becker, H.-J. Pohl, M. L. W. Thewalt, and S. Simmons, PRX Quantum **1**, 020301 (2020).
3. D. D. Awschalom, R. Hanson, J. Wrachtrup, and B. B. Zhou, Nat. Photonics **12**, 516 (2018).
4. M. Rančić, M. P. Hedges, R. L. Ahlefeldt, and M. J. Sellars, Nat. Phys. **14**, 50 (2018).
5. E. Miyazono, I. Craiciu, A. Arbabi, T. Zhong, and A. Faraon, Opt. Express **25**, 2863 (2017).
6. M. Raha, S. Chen, C. M. Phenicie, S. Ourari, A. M. Dibos, and J. D. Thompson, Nat. Commun. **11**, 1605 (2020).
7. A. J. Kenyon, Semicond. Sci. Technol. **20**, R65 (2005).
8. H. Przybylinska, W. Jantsch, Y. Suprun-Belevitch, M. Stepikhova, L. Palmetshofer, G. Hendorfer, A. Kozanecki, R. J. Wilson, and B. J. Sealy, Phys. Rev. B **54**, 2532 (1996).
9. C. M. Dodson and R. Zia, Phys. Rev. B **86**, 125102 (2012).
10. T. Asano and S. Noda, Proc. IEEE **106**, 2183 (2018).